

Effects of time-delayed feedback on the properties of self-sustained oscillators

S. Risau-Gusman

Centro Atómico Bariloche, 8400 S. C. de Bariloche, Argentina and Consejo Nacional de Investigaciones Científicas y Técnicas, Argentina

(Received 31 May 2016; revised manuscript received 22 September 2016; published 18 October 2016)

Most self-sustained oscillations in biological systems and in technical applications are based on a feedback loop, and it is usually important to know how they will react when an external oscillatory force is applied. Here we investigate the effects that the introduction of a time delay in the feedback can have in the entrainment properties of self-sustained oscillators. To do this, we derive analytic expressions for the periodic trajectories and their asymptotic stability, for a generic external oscillatory force. This allows us to show that, for large quality factors, the resonance frequency does not depend on the feedback delay. When the external force is harmonic, it is shown that the largest entrainment range does not correspond to the time delay that gives the maximal response of the unforced oscillator. In fact, that delay gives the shortest entrainment range.

DOI: [10.1103/PhysRevE.94.042212](https://doi.org/10.1103/PhysRevE.94.042212)

I. INTRODUCTION

Systems that display self-sustained oscillations are common in a wide range of domains. In electronics, oscillators are an essential part of many telecommunication devices [1]. Most of the designs include a resonator and a nonlinear feedback loop (see, e.g., [1–3]), and it has been shown that the introduction of a time delay in the signal that is reinjected to the resonator can have some interesting effects [4,5]. In biology, it is now well known that daily, or circadian, rhythms of the body are generated by the population oscillation of specific proteins inside cells [6]. Even though these cellular oscillations can be autonomous, they are also entrained by light and other environmental cues [7]. The basic mechanism of these cellular clocks is a negative feedback loop where a protein inhibits its own transcription. However, a time delay is necessary in these systems to achieve an oscillation lasting a whole day, because the cellular processes involved are much faster.

Given the complexity inherent to physical systems (be they micromechanical oscillators or clock neurons), it is always useful to have simple models that display the more important features of more complex systems. Unfortunately, the combination of nonlinearity and feedback makes it rather difficult to obtain analytical results for most simple systems. One is therefore forced to use approximation techniques [8], which in general implies restricting the analysis to some special cases (such as, for example, harmonic solutions, or small values of the forcing, or frequencies close to the natural frequency of the system, etc.). In this context, exactly solvable systems, although very simple, can be useful to get a more complete picture of the performance of self-sustained oscillators in various settings.

The system that we analyze here is a simplification, and a limit case, of the schematic design shown in Fig. 1. It consists of a resonator whose output signal is modified (through differentiation and time shifting) and then fed into an amplifier, after which it is reinjected to the resonator. This accounts for the possibility of a time-shifted feedback given by the signal (when the differentiator element is not present) or its derivative. We assume that the amplifier has a finite saturation level and an arbitrarily large gain. In this limit, the signal reinjected to the resonator takes only two values, given by the saturation of the amplifier. This type of feedback is well

known in engineering, where it is called *relay feedback* [9], and many analytical results are available for such systems. Here we extend those results to the case of an oscillator driven by an arbitrary periodic signal and with a feedback with a given time delay.

In the next section, we present the model and study in some detail the case of delayed feedback without a driving force. In Sec. IV we add an external force and determine the conditions that the parameters must satisfy for the system to be entrainable (in frequency) by this force. To achieve this, we calculate the asymptotic stability of those periodic trajectories of the system with the same period as the driving. Afterward, we add a delay to the feedback and show how this changes the parameter region where the system can be effectively entrained. All this is applied to the analysis of a particular example, a harmonic external force. Results are discussed and summarized in the final section.

II. MODEL OF A DELAYED FEEDBACK OSCILLATOR

The oscillator model we consider is an underdamped harmonic oscillator of one degree of freedom [$x(t)$] with a delayed nonlinear feedback, driven by a periodic signal. Its evolution is given by the equation

$$m\ddot{x} + \gamma\dot{x} + kx = F \operatorname{sgn}[y(t - \tau)] + F_1 f(t), \quad (1)$$

where $\operatorname{sgn}[\cdot]$ is the sign function, and $f(t)$ is an arbitrary periodic function with period $T_1 = 2\pi/\omega_1$. The functional form of $y(t)$ defines the type of feedback. We consider here two possibilities: $y(t) = x(t)$ or $y(t) = \dot{x}(t)$. In the rest of the paper, these two different feedback mechanisms will be called *position* and *velocity* feedback, respectively. Performing the rescalings $kx \rightarrow x$, $t\sqrt{k/m} \rightarrow t$, Eq. (1) can be rewritten as

$$\ddot{x} + Q^{-1}\dot{x} + x = F \operatorname{sgn}[y(t - \tau)] + F_1 f(t), \quad (2)$$

where $Q > 1/2$ is the *quality factor* of the oscillator, defined as $Q = \sqrt{km}/\gamma$. F could be absorbed into F_1 , but we leave it undisturbed because it is necessary to differentiate between positive and negative feedbacks. Equation (2), in turn, can be more compactly rewritten as

$$\dot{\mathbf{x}} = \mathbf{A}\mathbf{x} + \mathbf{b}(t, \tau), \quad (3)$$

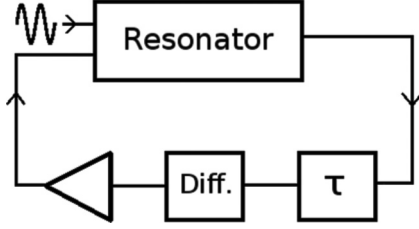


FIG. 1. Schematic diagram of a feedback oscillator. The triangular box represents an amplifier, and the square boxes to its right represent a differentiator and a time shifter. The resonator is also fed with a periodic signal (the driving).

with

$$\mathbf{A} = \begin{bmatrix} -Q^{-1} & -1 \\ 1 & 0 \end{bmatrix}, \quad (4)$$

$$\mathbf{b}(t, \tau) = (F \operatorname{sgn}[y(t - \tau)] + F_1 f(t), 0)^T,$$

$\mathbf{x} = (\dot{x}(t), x(t))^T$, $y(t) = \mathbf{c} \cdot \mathbf{x}(t)$, and $\mathbf{c} = (1, 0)$ for velocity feedback, or $\mathbf{c} = (0, 1)$ for position feedback.

Given an initial time t_i , we define the *switching times* $t_1 < t_2 < \dots < t_n$ (with $t_i < t_k < t$ for $k = 1, 2, \dots$) as the times when $y(t)$ changes sign. Between $t_k + \tau$ and $t_{k+1} + \tau$, the system is subject to the dynamics of an underdamped forced oscillator, with a constant term that can be either F or $-F$. The full solution can thus be obtained by simply pasting together solutions of the underdamped forced oscillator at $t_k + \tau$ ($k = 1, 2, \dots$). If $\tau \geq 0$, in order to specify an initial condition it is enough to give $\mathbf{x}(t_i)$ and a set of times $t_{-n'} < \dots < t_0$ (with $t_i - \tau < t_{-k} \leq t_i$ for $k = 0, 1, 2, \dots$) at which $y(t)$ vanishes. Using this, the solution to Eq. (3) can be written, formally, as

$$\begin{aligned} \mathbf{x}(t) &= e^{\mathbf{A}(t-t_i)} \mathbf{x}(t_i) + \int_{t_i}^t e^{\mathbf{A}(t-u)} \mathbf{b}(u, \tau) du \\ &= e^{\mathbf{A}(t-t_i)} \mathbf{x}(t_i) + F_1 \int_{t_i}^t e^{\mathbf{A}(t-u)} \mathbf{c}^T f(u) du \\ &\quad + 2Fs e^{\mathbf{A}(t-\tau)} \sum_{k=-n'+1}^{n_i} (-1)^k e^{-\mathbf{A}t_k} \mathbf{A}^{-1} \mathbf{c}^T \\ &\quad + Fs [(-1)^{n_i+1} e^{-\mathbf{A}(t-t_i)} + (-1)^{n'} \mathbf{I} \mathbf{A}^{-1} \mathbf{c}^T, \end{aligned} \quad (5)$$

where \mathbf{I} is the 2×2 identity matrix. s is the sign of $y(t_i^+)$, thus if t_i is not a switching time, we have $s = \operatorname{sgn}[y_i(t_i)]$, whereas if t_i is a switching time, we have $s = -\operatorname{sgn}[(0, 1) \cdot \mathbf{x}_i(t_i)]$ for velocity feedback or $s = \operatorname{sgn}[(1, 0) \cdot \mathbf{x}_i(t_i)]$ for position feedback. n is the largest integer such that $t_n + \tau < t$, and it can even be negative if $t < t_i + \tau$.

Equation (5), the solution to Eq. (3), is only formal because one needs to know the switching times t_1, \dots, t_n in advance. To obtain them, Eq. (5) must be used recursively. We use first the switching times of the initial condition and Eq. (5) to find all the times in the interval $(t_i, t_i + \tau]$ at which $y(t)$ changes sign. Next we add these times to the list of switching times, and we calculate all the times in the interval $(t_i + \tau, t_i + 2\tau]$ at which $y(t)$ changes sign, which are then added to the list. By applying this procedure iteratively, one finds all the switching times that are necessary for a complete solution of Eq. (3). If

$\tau = 0$, at each step we simply find the smallest time $t_{k+1} > t_k$ (where t_k is the switching time found in the previous step) at which $y(t)$ changes sign and update the list.

III. OSCILLATIONS WITHOUT EXTERNAL FORCING

When $F_1 = 0$, these systems fall into the category of relay feedback systems [9,10], which can be shown to have limit cycles. As mentioned above, in the intervals $(t_k + \tau, t_{k+1} + \tau)$ ($k = 1, 2, \dots$) the system behaves as an underdamped oscillator whose solution is a sinusoidal function of angular frequency $\omega = \sqrt{1 - (2Q)^{-2}}$, with an amplitude that decays exponentially. Thus, consecutive zeros of $x(t)$ are always separated by a distance of $T/2 = \pi/\omega$, and the same happens with the zeros of $\dot{x}(t)$. This implies that, when $\tau = 0$, if the oscillator described by Eq. (2) has a limit cycle, its period must necessarily be T (as happens with other oscillators whose switching dynamics also depends on the zeros of the velocity or the position [11]). But, if $\tau \neq 0$ this is no longer the case, because at the moment when the dynamics changes, neither the value of $x(t)$ nor the value of $\dot{x}(t)$ vanishes. Figure 2 shows some examples of the solution of Eq. (2) and the corresponding limit cycles for different values of the feedback delay.

We will concentrate here on *antiperiodic* limit cycles of period T_τ , defined as those that satisfy $\mathbf{x}^*(t + T_\tau/2) = -\mathbf{x}^*(t)$, and which have only two switching times per cycle (the case with more switching times is more difficult to analyze and seems to appear much less frequently in the simulations). This condition implies that $T_\tau/2 \leq T/2 + \tau$. We first consider the case of τ small enough so that any time interval of length τ contains at most one switching time. This implies both that $\tau < T/2$ and $\tau < T_\tau/2$. Let the initial time t_i be a switching time, and let $s = 1$. Using Eq. (5) and enforcing the

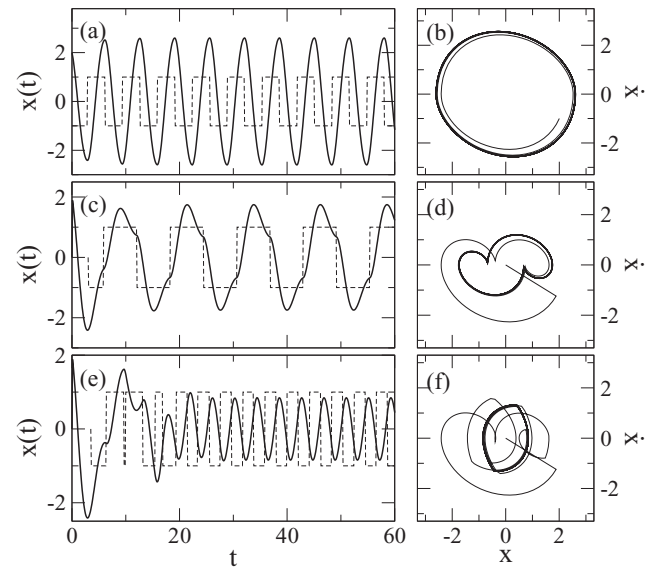


FIG. 2. Examples of time series (left panels) and phase portraits (right panels) of an oscillator with velocity feedback, $Q = 2$, $F = 1$, and $F_1 = 0$, for some values of the delay τ . Dashed lines in the left panels represent the switching function $\operatorname{sgn}[y(t - \tau)]$. Thick black lines in the right panels represent limit cycles. (a) and (b) $\tau = 0.2$, (c) and (d) $\tau = 3.0$, (e) and (f) $\tau = 3.4$.

antiperiodicity condition, we obtain the value of $\mathbf{x}_0^* \equiv \mathbf{x}^*(t_i)$ [10],

$$\mathbf{x}_0^* = F[\mathbf{I} - 2(e^{-AT_\tau/2} + \mathbf{I})^{-1}e^{-A\tau}]\mathbf{A}^{-1}\mathbf{c}^T. \quad (6)$$

\mathbf{x}_0^* does not depend explicitly on t_i because the system is autonomous. To find the period of the limit cycle, we use now that t_i is a switching time and must thus satisfy

$$\mathbf{c} \cdot \mathbf{x}_0^* = 0 \quad (7)$$

and solve this equation for T_τ . Note that the condition that the limit cycle has only two switches per cycle is not necessarily satisfied by all the solutions of Eq. (7), and it must be separately enforced. Once T_τ and \mathbf{x}_0^* have been found, plugging them into Eq. (5) gives the exact equation for the limit cycle for all t . In particular, it is generally useful to calculate the *amplitude* of the limit cycle, defined as the largest value of the position coordinate.

For the family of models considered here, the case of velocity feedback leads to particularly simple equations. In the following, emphasis will be put on the properties of systems with this type of feedback, but analogous results for position feedback will also be mentioned. For $\tau < T/2$, the equation for T_τ becomes

$$h_0(T_\tau) = 0 \quad (8)$$

with

$$h_0(T_\tau) = \sin[\omega\tau] + e^{T_\tau/4Q} \sin[\omega(\tau - T_\tau/2)]. \quad (9)$$

As mentioned above, the fact that between switchings the system is subject only to the dynamics of an underdamped harmonic oscillator implies that $\tau \leq T_\tau/2 \leq T/2 + \tau$. In this range, Eq. (8) has only two solutions, one corresponding to the case with $F > 0$ (negative feedback) and the other to $F < 0$ (positive feedback).

This can be generalized to larger values of the delay. When $nT/2 \leq \tau \leq (n+1)T/2$ ($n = 1, 2, \dots$), any time interval of length τ can contain only n or $n+1$ switching times. To find the period of the limit cycle, we assume again that in the interval $(t_i - \tau, t_i - \tau + T_\tau/2)$ there is only one switching time, $t_{-n} = t_i - nT_\tau/2$. We get then the same equations as in the last paragraph, but replacing τ by $\tau - nT_\tau/2$. In particular, the equation for T_τ is now

$$\sin[\omega(\tau - nT_\tau/2)] + e^{T_\tau/4Q} \sin[\omega[\tau - (n+1)T_\tau/2]] = 0. \quad (10)$$

The condition that there are only two switching times per period implies now that T_τ must satisfy $\tau - nT_\tau/2 \leq T_\tau/2 \leq T/2 + \tau - nT_\tau/2$. Within this range, Eq. (10) has only two solutions, which are shown in Fig. 3 for some values of Q . The corresponding amplitudes are shown in Fig. 4. Note that both the period and the amplitude change abruptly when the delay is a multiple of $T/2$. This reflects an abrupt change in the shape of the limit cycle (compare the two lower panels of Fig. 2).

When the feedback is delayed, the amplitude of the signal can never be larger than A_{\max} , the amplitude for the system with no delay, given by

$$A_{\max} = F \frac{\exp(T/4Q) + 1}{\exp(T/4Q) - 1}. \quad (11)$$

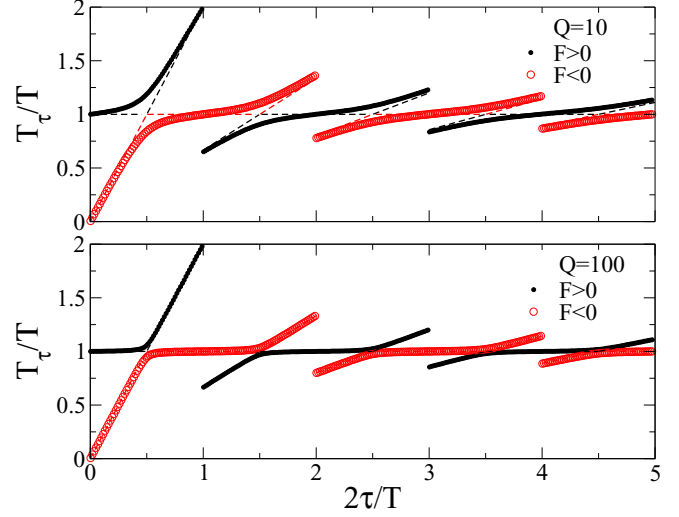


FIG. 3. Period of the limit cycle for systems with velocity feedback, as a function of the delay for two different values of the quality factor. The dotted lines show \tilde{T}_τ , the approximation for large Q values [Eq. (13)].

This is approximately proportional to Q in the limit of large Q .

In the following, we will focus on delays that satisfy $\tau < T/2$. In this range, the minimal value of the amplitude is

$$A_{\min} = F \frac{[\exp(T/4Q) + 1]^2}{\exp(T/2Q) + 1}. \quad (12)$$

Note that this value depends only very weakly on Q : it is always between F and $2F$.

In the case of systems with position feedback, if $F > 0$, Eq. (1) has a fixed point at $x(t) = F$. However, $F < 0$ does lead to oscillations for all values of the delay. Figure 5 shows the period and amplitude of the resulting signal. Note that what

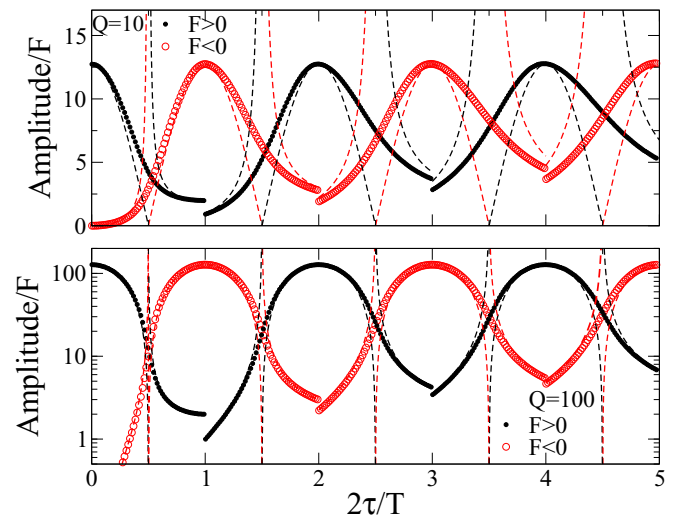


FIG. 4. Amplitude of the limit cycle for systems with velocity feedback, as a function of the delay for two different values of the quality factor. The dotted lines show \tilde{A}_τ , the approximation for large Q values [Eq. (14)].

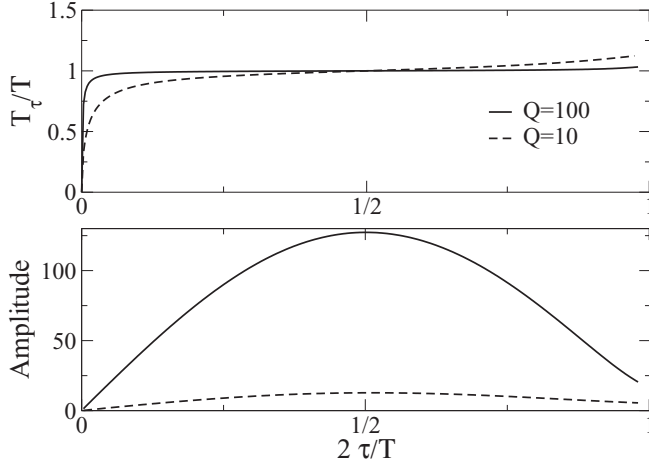


FIG. 5. Period (upper panel) and amplitude (lower panel) of the limit cycle for systems with position feedback and $F = 1$, as a function of the delay for two different values of the quality factor.

is obtained with a feedback containing $x(t - \tau)$ is very similar to what is obtained with a feedback containing $\dot{x}(t - \tau + \pi/2)$ (and $F > 0$), as happens when a harmonic approximation is used [12].

A. Large- Q limit

It is instructive to consider what happens in the limit of large Q for velocity feedback. In this limit, $\omega = 1 + O(Q^{-2})$, $T = 2\pi + O(Q^{-2})$, and it can be shown that Eq. (10) has two solutions of the form $T_\tau = \tilde{T}_\tau + O(Q^{-1})$, with

$$\tilde{T}_\tau = \begin{cases} 2\pi, & n - \frac{1}{2} \leq \frac{\tau}{\pi} \leq n + \frac{1}{2}, \\ \frac{4\tau}{2n+1}, & n + \frac{1}{2} \leq \frac{\tau}{\pi} \leq n + 1, \\ \frac{4\tau}{2n+3}, & n + 1 < \frac{\tau}{\pi} \leq n + \frac{3}{2}, \end{cases} \quad (13)$$

where $n = 1, 3, 5, \dots$ if $F < 0$, and $n = 0, 2, 4, \dots$ if $F > 0$ (for $n = 0$, replace $n - 1/2$ by 0). Using this, the amplitude for large Q is $A_\tau = \tilde{A}_\tau + O(Q^{-1})$, with

$$\frac{\tilde{A}_\tau}{F} = \begin{cases} \frac{4Q}{\pi} \cos \tau, & n - \frac{1}{2} \leq \frac{\tau}{\pi} \leq n + \frac{1}{2}, \\ 1 - [\cos(\frac{\tau}{2n+1})]^{-1}, & n + \frac{1}{2} \leq \frac{\tau}{\pi} < n + 1, \\ 1 - [\cos(\frac{\tau}{2n+3})]^{-1}, & n + 1 \leq \frac{\tau}{\pi} < n + \frac{3}{2}, \end{cases} \quad (14)$$

using the same convention for τ as in the previous equation. This shows that when Q is large, there are two very different regimes for this oscillator. In one of them, the period coincides with the damped period of the system, and it does not depend on the amount of delay. On the other hand, the amplitude is proportional to the quality factor and changes substantially as the delay is modified, reaching a maximum at $\tau = n\pi$ with $n = 0, 1, 2, \dots$ if $F > 0$, and $n = 1, 3, 5, \dots$ if $F < 0$. In the other regime, the period of oscillation becomes linearly dependent on τ , and the amplitude becomes much smaller and no longer depends on Q . Within this small-amplitude regime, there is a discontinuity for both the period and the amplitude at $\tau = n\pi$ with $n = 0, 1, 2, \dots$ if $F < 0$, and $n = 1, 3, 5, \dots$ if $F > 0$. Figures 3 and 4 show that this limit is a good approximation

for $Q > 100$, except for the delay values where there is a crossover between the two regimes.

B. Stability

Even though for all parameter values there are limit cycles in the systems we consider, it is not necessarily true that they are relevant for the dynamics of the system. One step in this direction is determining whether limit cycles are asymptotically locally stable [13]. Considering a trajectory with a small deviation from the position of the limit cycle at a switching time (\mathbf{x}_0^*), and performing a linear approximation to calculate the deviation from the position of the limit cycle at the next switching time, one can calculate \mathbf{W} , the Jacobian of the resulting Poincaré map, which gives [10]

$$\mathbf{W} = \left(\mathbf{I} - \frac{(\mathbf{A}\mathbf{x}_0^* + F\mathbf{e}_1)\mathbf{c}}{\mathbf{c}(\mathbf{A}\mathbf{x}_0^* + F\mathbf{e}_1)} \right) e^{AT_\tau/2}, \quad (15)$$

where $\mathbf{e}_1 = (1, 0)^T$, and \mathbf{x}_0^* is given by Eq. (6). The condition for local stability is that this matrix has eigenvalues of absolute value smaller than 1. But one of the eigenvalues always vanishes (it corresponds to the left eigenvector \mathbf{c}). Thus, the condition for stability can be given simply in terms of the trace of \mathbf{W} . If we specialize to systems with velocity feedback, the condition for stability is

$$g(T_\tau/2)e^{-T_\tau/4Q} < 1 \quad (16)$$

with

$$g(t) = \cos(\omega t) + (2\omega Q)^{-1} \sin(\omega t). \quad (17)$$

Interestingly, a bit of calculus shows that this condition is fulfilled for all non-negative values of the constants. In other words, limit cycles are always locally asymptotically stable. Furthermore, simulations suggest that this stability can be global (we have not found a single initial condition for which the system does not end arbitrarily close to the limit cycle).

IV. EXTERNAL FORCING WITH A PERIODIC SIGNAL

We turn now to the analysis of an oscillator forced by an external periodic signal of period T_1 . For simplicity, we concentrate in the following on external antiperiodic functions [i.e., functions that satisfy $f(x + T_1/2) = -f(x)$]. As in the previous section, we consider here solutions that are symmetric and have only two switchings per cycle. We define the system as *entrained* if there is a limit cycle with period T_1 (this is also known as frequency locking [14]). To find these limit cycles, we proceed as in the previous section, but replacing T_τ by T_1 everywhere. We define again t_i as a switching time of the limit cycle. Defining $\mathbf{x}^* \equiv \mathbf{x}^*(t_i)$, and using the symmetry condition [$\mathbf{x}^*(t_i + T_1/2) = -\mathbf{x}^*(t_i)$], we obtain

$$\mathbf{x}^* = -F_1(e^{-AT_1/2} + \mathbf{I})^{-1} \int_0^{T_1/2} e^{-\mathbf{A}u} \mathbf{c}^T f(u + t_i) du + F[\mathbf{I} - 2(e^{-AT_1/2} + \mathbf{I})^{-1} e^{-\mathbf{A}\tau}] \mathbf{A}^{-1} \mathbf{c}^T. \quad (18)$$

To obtain the full solution for the limit cycle, we need to find one switching time t_i , which in this case is not arbitrary because the forced system is nonautonomous (in other words,

the phase of the external signal determines the phase of the solution of the system). To do this, we solve the equation for the switching time condition,

$$\mathbf{c} \cdot \mathbf{x}^* = 0, \quad (19)$$

with t_i as the only unknown. We are interested now in finding, in parameter space, the region of existence, i.e., the parameter sets for which this equation has a solution. In particular, we focus here on the region of existence in the plane (ω, F_1) , for fixed values of Q and τ . Generally, it can be shown that for a given Q there is a solution if F_1 is large enough. Conversely, it is intuitively clear that there should be a threshold for F_1 , below which there can be no entrainment.

A. Existence of entrained trajectories

To determine the conditions that must be satisfied by the parameters for the existence of entrainment, it is useful to rewrite Eq. (19) as

$$\omega F_1 h_1(t_i) = 2F e^{(\tau - T_1/2)/2Q} h_0(T_1) \quad (20)$$

with

$$h_1(t_i) = \int_0^{T_1/2} f(u + t_i) e^{u/2Q} [g(u - T_1/2) + e^{-T_1/4Q} g(u)] du, \quad (21)$$

and $h_0(T_1)$ and $g(u)$ defined as in Eqs. (9) and (17), respectively. If $f(t)$ is a piecewise continuous function, then $h_1(t_i)$ is a continuous function of t_i , and therefore it reaches a maximum and a minimum in the interval $[0, T_1/2]$ at $t_i = t_{\max}$ and t_{\min} , respectively. Furthermore, $h_1(t_{\max}) > 0$ and $h_1(t_{\min}) < 0$, because of the antiperiodicity of $f(t)$. Thus, if all other parameters are fixed, Eq. (20) can only have a solution when $F_1 \geq h_0(T_1)/h_1(t_{\max})$ [if $h_0(T_1) > 0$] or $F_1 \geq h_0(T_1)/h_1(t_{\min})$ [if $h_0(T_1) < 0$].

In the limit of infinite Q , it is clear that $h_1(t_i) \rightarrow 0$ when $T_1 \rightarrow 2n\pi$ with n odd, but, as we also have $h_0(T_1) \rightarrow 0$, whether or not F_1 diverges at these values will depend on the exact form of the driving function. Other possible divergences for F_1 are the values of T_1 for which $h_1(0) = 0$ because this could imply that either $h_1(t_{\max}) = 0$ or $h_1(t_{\min}) = 0$. Again, this will depend on the exact form of $f(t)$. For all other values of T_1 , F_1 will be bounded, as a function of Q . Equation (9) implies that $h_0(T_1)$ vanishes when T_1 coincides with the period for the unforced system, and therefore entrained trajectories exist for every value of F_1 in that case.

Taking all this into account, we can infer the general form of the existence curve for F_1 [i.e., the curve above which Eq. (20) has a solution] for fixed τ and large Q . It has zeros where T_1 is a solution of Eq. (8) and it may have some barriers with a height given by an increasing function of Q , with deep valleys between barriers. For all other values of T_1 , the critical values of F_1 may grow with Q but are nevertheless bounded. An important caveat is that it can happen that the solutions have more than a switching per period, and thus they are not acceptable. One should then calculate a second existence curve delimiting the region where the solutions have only one switching point. Simulations seem to show that it is only around the zeros that this second curve is above the existence curve (see the next section).

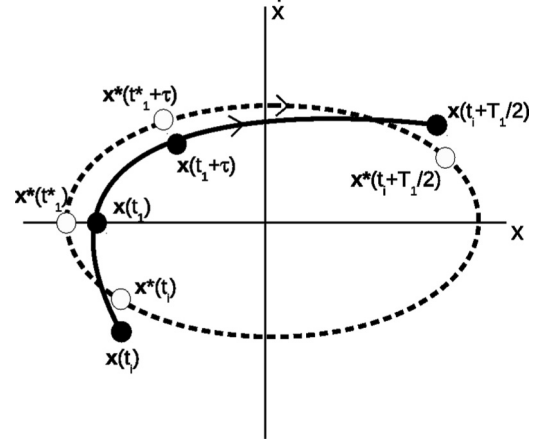


FIG. 6. Illustration of a trajectory (full line) of a velocity-based feedback oscillator in phase space that is close to a periodic trajectory (dotted line).

In the regime where the system has entrained periodic trajectories, it is important to know where the resonances are, i.e., the frequencies at which the amplitude has a maximum. In particular, we look for sharp maxima with a height that is proportional to the quality factor Q . From Eq. (18) it can be shown that, in the limit of very large Q , sharp maxima in the amplitude can only appear when $(e^{-AT_1/2} + \mathbf{I})^{-1}$ diverges. But this matrix can be written as

$$(e^{-AT_1/2} + \mathbf{I})^{-1} = \frac{e^{T_1/4Q} (e^{-T_1/2Q} \mathbf{I} + e^{AT_1/2})}{2[\cosh(T_1/4Q) + \cos(\omega T_1/2)]}, \quad (22)$$

which can only diverge where the denominator vanishes. It is then straightforward to check that, for large Q , resonances can only appear for $T_1 = 2\pi n$ with $n = 1, 3, 5, \dots$. Note that this implies that even when the feedback is delayed, the resonances depend mainly on the natural frequency of the system (when Q is large, $\omega \approx 1$), and only weakly on τ . An example of this is shown in Sec. IV C.

B. Stability of entrained trajectories

To study the stability of the periodic trajectories that determine the entrainment of the system, we calculate the stability of the map, $\mathbf{x}(t) \rightarrow \mathbf{x}(t + T_1/2)$, as a function of the initial vector \mathbf{x}_i at the initial time t_i . Let $\mathbf{x}^*(t)$ be a periodic orbit and $\mathbf{x}(t)$ a trajectory of the system for an arbitrary initial condition. We assume that $\dot{x}(t_i) < 0$ for velocity feedback [$x(t_i) < 0$ for position feedback], and that at t_i the system is so close to the periodic trajectory that it can be guaranteed that there is exactly one switching time between t_i and $t_i + T_1/2$. We call this switching time t_1 and we call t_1^* the first switching time of the periodic trajectory after t_i (see Fig. 6). Furthermore, we will also assume that $t_i > t_1^* + \tau - T_1/2$, which forces us to use an initial function that has no switching time, if we want an initial state that is very close to the periodic trajectory. The times t_1 and t_1^* can be obtained by solving the equations $\mathbf{c} \cdot \mathbf{x}^*(t_1^*) = 0$ and $\mathbf{c} \cdot \mathbf{x}(t_1) = 0$, which can be

written as

$$\mathbf{0} = \mathbf{c}e^{\mathbf{A}(t_1^* - t_i)} \left[\mathbf{x}^*(t_i) + \int_0^{t_1^* - t_i} e^{-\mathbf{A}u} \mathbf{b}_-(u + t_i) du \right], \quad (23)$$

$$\mathbf{0} = \mathbf{c}e^{\mathbf{A}(t_1 - t_i)} \left[\mathbf{x}(t_i) + \int_0^{t_1 - t_i} e^{-\mathbf{A}u} \mathbf{b}_-(u + t_i) du \right],$$

where $\mathbf{b}_-(t) = F_1 f(t) - F$. After half a period, the difference between the trajectories becomes

$$\begin{aligned} & \mathbf{x}(t_i + T_1/2) - \mathbf{x}^*(t_i + T_1/2) \\ &= e^{\mathbf{A}(T_1/2)} [\mathbf{x}(t_i) - \mathbf{x}^*(t_i)] \\ &+ \int_{t_1 + \tau}^{t_1^* + \tau} e^{\mathbf{A}(t_i + T_1/2 - u)} [\mathbf{b}_-(u) - \mathbf{b}_+(u)] du, \end{aligned} \quad (24)$$

where $\mathbf{b}_+(t) = F_1 f(t) + F$. Combining Eqs. (23) and (24), we obtain

$$\mathbf{x}(t_i + T_1/2) - \mathbf{x}^*(t_i + T_1/2) = \mathbf{H}[\mathbf{x}(t_i) - \mathbf{x}^*(t_i)] \quad (25)$$

with

$$\begin{aligned} \mathbf{H} &= e^{\mathbf{A}(T_1/2)} (\mathbf{I} + e^{\mathbf{A}\tau} \mathbf{W}), \\ \mathbf{W} &= \frac{2F [e^{\mathbf{A}(t_i - t_1^*)} - e^{\mathbf{A}(t_i - t_1)}] \mathbf{A}^{-1} \mathbf{c}^T \mathbf{c} e^{\mathbf{A}(t_1 - t_i)}}{\mathbf{c} [(\mathbf{I} - e^{\mathbf{A}(t_1 - t_1^*)}) \mathbf{x}^*(t_1^*) + \int_{t_1}^{t_1^*} e^{\mathbf{A}(t_1 - u)} \mathbf{b}_-(u) du]}. \end{aligned} \quad (26)$$

If we take the limit $\mathbf{x}_i \rightarrow \mathbf{x}^*(t_i)$ (i.e., the initial position of the system becomes very close to the periodic trajectory evaluated at the initial time), we have $t_1 \rightarrow t_1^*$. In this limit, \mathbf{W} becomes

$$\mathbf{W} = \frac{2F e^{\mathbf{A}(t_i - t_1^*)} \mathbf{c}^T \mathbf{c} e^{\mathbf{A}(t_1^* - t_i)}}{\mathbf{c} [\mathbf{A} \mathbf{x}^*(t_1^*) + \mathbf{b}_-(t_1^*)]} + O(|t_1 - t_1^*|). \quad (27)$$

Because all the matrices involved are 2×2 matrices, their eigenvalues can be obtained from the determinant and the trace. Using this property, it is straightforward to show that the eigenvalues of \mathbf{H} are the same as those of $\mathbf{H}^* = e^{\mathbf{A}(T_1/2)} (\mathbf{I} + \mathbf{W}^*)$ with

$$\mathbf{W}^* = \frac{2F \mathbf{c}^T \mathbf{c}}{\mathbf{c} [\mathbf{A} \mathbf{x}^*(t_1^*) + \mathbf{b}_-(t_1^*)]}. \quad (28)$$

Using \mathbf{H}^* , the conditions for asymptotic stability become independent from the initial time t_i . A given periodic trajectory will be asymptotically stable in the parameter region where both eigenvalues of \mathbf{H}^* are smaller than 1. Furthermore, when the eigenvalues are complex, the stability condition is simply given by $\det \mathbf{H}^* < 1$. For the case of oscillators with velocity feedback, this can be rewritten as

$$\frac{2F e^{\tau/Q} g(\tau)}{\mathbf{c} [\mathbf{A} \mathbf{x}^*(t_1^*) + \mathbf{b}_-(t_1^*)]} < e^{T_1/2Q} - 1. \quad (29)$$

C. External harmonic force and velocity feedback

As an example of the use of these formulas, we apply them to the analysis of a feedback oscillator driven by a harmonic force, $f(t) = \cos(\omega_1 t)$. The condition for the existence of

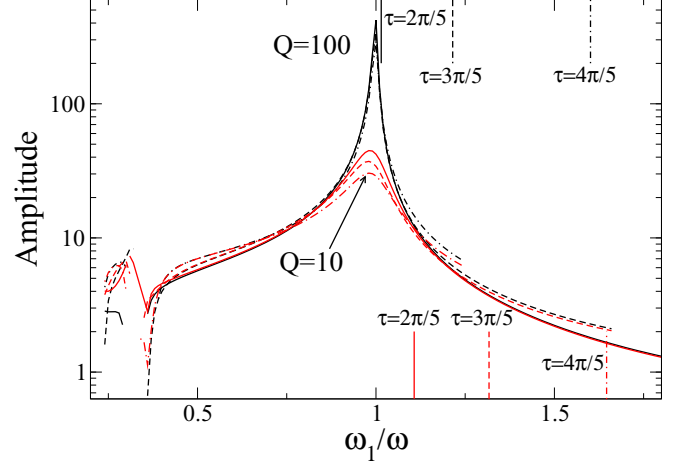


FIG. 7. Amplitude for an entrained oscillator with velocity delayed feedback and $F_1 = 4$. Upper, black curves correspond to $Q = 100$ and $\tau = 2\pi/5$, $\tau = 3\pi/5$, and $\tau = 4\pi/5$ (all coincide at the sharp peak). Lower, red curves correspond to $Q = 10$ and $\tau = 2\pi/5$, $\tau = 3\pi/5$, and $\tau = 4\pi/5$. Vertical lines mark the frequencies of oscillation for the corresponding unforced systems. In the vicinity of the predicted resonance at $\omega_1 = 1/3$ there is a break in the lines because for $F_1 = 4$ there is no entrainment at these values of ω_1 (these parameters fall inside the barriers of the corresponding existence curves).

solutions can be written as

$$F_1 < \frac{|h_0(T_1)| \sqrt{(\omega_1^2 - \omega^2)^2 + Q^{-2} [2(\omega_1^2 + \omega^2) + Q^{-2}]}}{|\cos(\omega T_1/2) + \cosh(T_1/4Q)|}. \quad (30)$$

This shows that for $\tau > 0$, the existence curve has maxima of height proportional to Q at $T_1 = 2\pi n$ with $n = 1, 3, 5, \dots$. In the case of $\tau = 0$, the existence curve has zeros at these values, which are surrounded by barriers of height proportional to Q (see the dashed lines in Figs. 8–11).

The calculation of the amplitude of the entrained solutions for this case shows that its dependence on the angular frequency of the external driving force is similar to what is observed in a harmonic oscillator. It is also apparent that the main resonance depends very weakly on τ for large Q . Already for $Q = 100$ the main resonance is the same (at $T_1 = T$) for all values of τ (see Fig. 7). The height of this resonance is proportional to Q , whereas the height of the other resonances is clearly much smaller.

Turning now to the stability of the entrained trajectories, we consider first the case of feedback without delay. Figures 8 and 9 show the regions in the parameter space of the driving force where the system can be entrained. These are the regions above the full curves, where at least one of the eigenvalues of \mathbf{H}^* is 1. Except for the peaks that are observed at $\omega_1 = \omega/2n$ with $n \in \mathbb{N}$, the rest of the curve is given by the condition $\det \mathbf{H}^*(t_1^*) = 1$. The peaks become very narrow as the quality factor is increased, and one can then assume that the stability region can be obtained by solving Eq. (29). In the general case, this condition gives a lower bound for the boundary of the stability region.

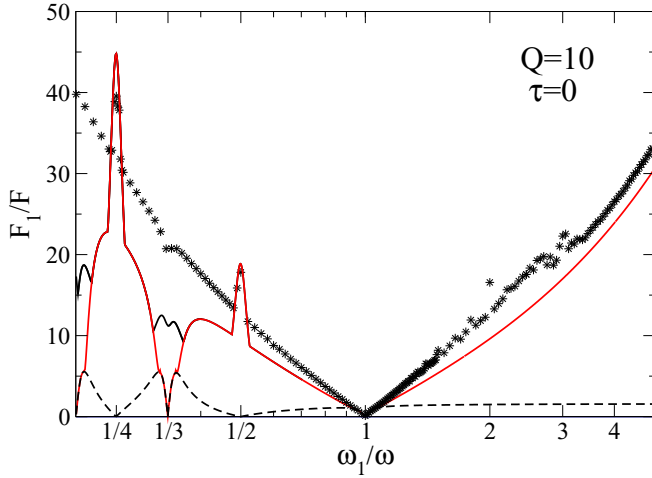


FIG. 8. Entrainment regions in the (ω_1, F_1) plane for a feedback oscillator with $Q = 10$, driven by a harmonic signal. The dotted line bounds the existence region of a periodic symmetric solution. Below the full red line, these solutions lose stability. The full black line indicates the values below which the system has no periodic solutions with only one switching per cycle. Stars represent results obtained from numerical simulations: with these parameter values, 90% of the systems converge to the periodic symmetric orbit (see the text for details).

A comparison between Figs. 8 and 9 shows that the external force has to be much stronger to drive an oscillator with a larger quality factor. Taking the limit of large Q and F_1 in Eq. (29), it can be shown that the dependence of the critical value of F_1 with the quality factor is $F_1^{\text{crit}} \approx Q$. The figures also show that the stability curve has a pronounced drop at $\omega_1/\omega = 1/n$ with $n = 1, 3, 5, \dots$. This happens because these values are close to the resonances mentioned at the end of Sec. IV A, which implies that limit cycles have a large amplitude for all values of F_1 , which in turn implies [see Eq. (29)] that a small value of F_1 is enough for the stability of these solutions.

To understand whether asymptotic stability results are relevant for the dynamics of the system, we have resorted to

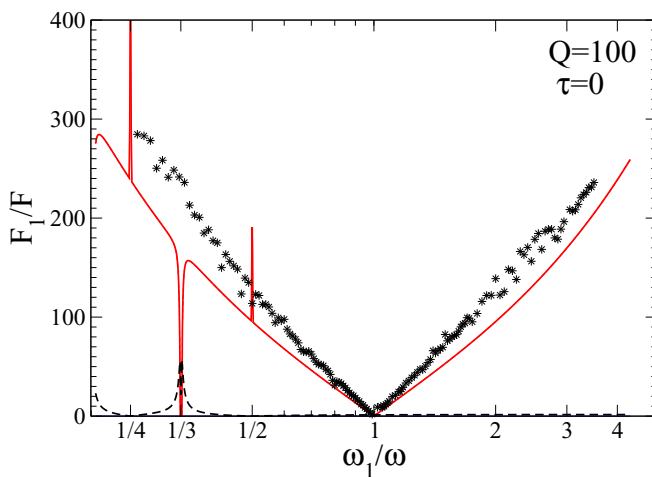


FIG. 9. Entrainment regions in the (ω_1, F_1) plane for a feedback oscillator with $Q = 100$. Conventions are the same as in Fig. 8.

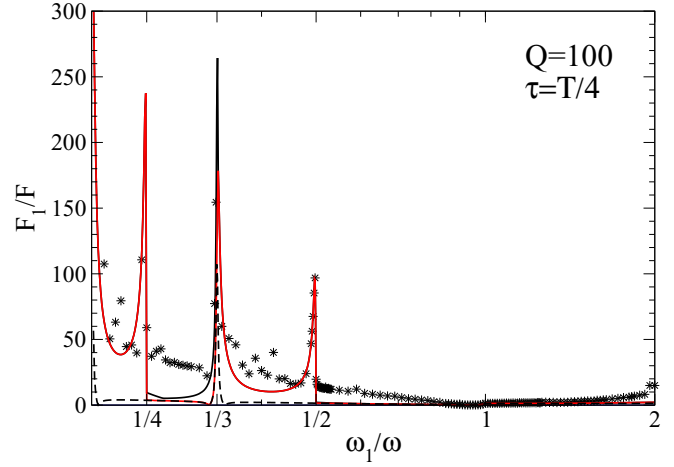


FIG. 10. Entrainment regions in the (ω_1, F_1) plane for a delayed-feedback oscillator with $Q = 100$ and $\tau = T/4$. Conventions are the same as in Fig. 8.

numerically solving Eq. (2) with different initial conditions. These were chosen at random from a cube of size $2|\mathbf{x}^*(t_i)|$ centered at $\mathbf{x}^*(t_i)$, where $\mathbf{x}^*(t_i)$ is the coordinate vector of the predicted limit cycle and t_i one of its switching times. After a time between $100T_1$ and $500T_1$, we evaluated whether the system was converging to the limit cycle given by Eq. (18). The results of these simulations are represented in Figs. 8 and 9. The stars represent the parameter values for which 90% of the systems converge to the periodic trajectories. Their relative closeness to the stability curve shows that the basin of attraction of the periodic trajectories is reasonably large.

In the previous section, it has been shown that introducing a delay in the feedback leads to a system with a smaller response, and this effect is maximal when the delay is equal to a quarter of the damped period. On the other hand, when the same system is forced by a harmonic signal, the entrainment range (i.e., the region enclosed by the boundaries of the stability region) is much larger than in the system with no delay in its feedback

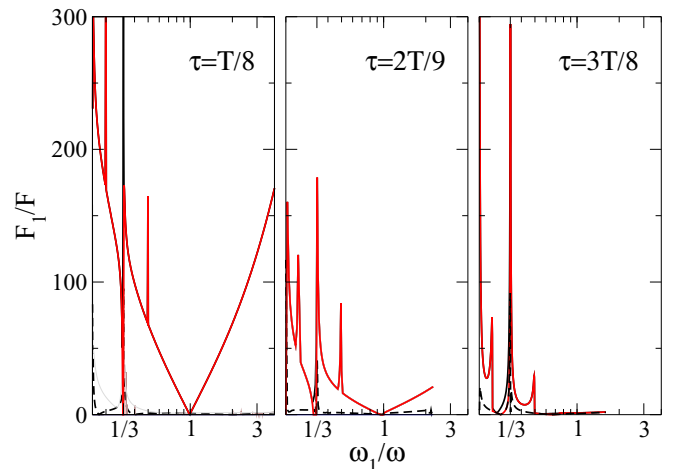


FIG. 11. Entrainment regions in the (ω_1, F_1) plane for three delayed-feedback oscillators with $Q = 100$ and different values for the delay. Conventions are the same as in Fig. 8.

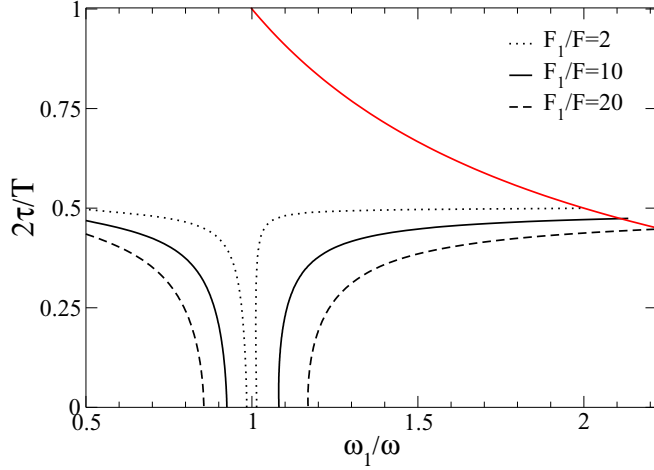


FIG. 12. Entrainment regions in the (ω_1, τ) plane for an oscillator with velocity feedback for $Q = 100$. The entrainment region for oscillators with $F_1 = 2F$, $F_1 = 10F$, and $F_1 = 20F$ lies between the upper red curve and the black stability curves corresponding to $F_1 = 2F$, $F_1 = 10F$, and $F_1 = 20F$, respectively. The upper red curve represents the values for which τ equals a semiperiod of the driving force.

(see Fig. 10). In fact, the presence of any amount of delay enlarges the stability zone, as Fig. 11 shows. Furthermore, when the delay is larger than $T/4$, the stability region is almost as large as in the case of $\tau = T/4$.

To quantify this dependence on τ of the stability region, we fixed the value of F_1 and solved the stability equations for τ for each value of ω_1 . The resulting curves (Fig. 12) show clearly that for fixed τ , the entrainment range grows with τ and is maximal for $\tau = T/4$. This dependence can be understood, at least for large Q and F_1 , by using again Eq. (29). $g(\tau)$, in the numerator on the left-hand side, is a decreasing function that becomes negative when $\tau \gtrsim T/4 + 1/2Q$ (we only consider

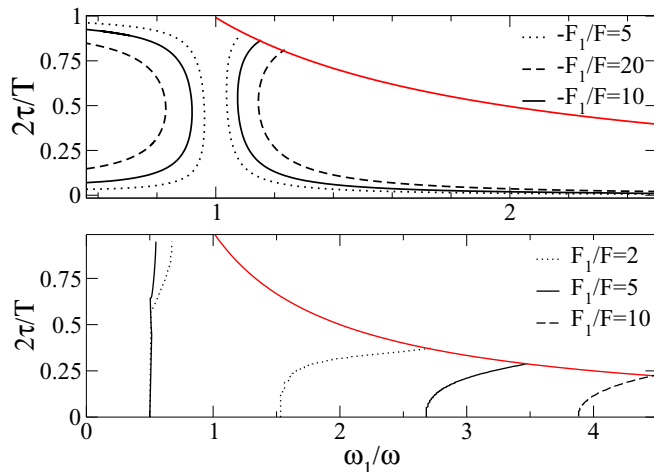


FIG. 13. Entrainment regions in the (ω_1, τ) plane for an oscillator with position feedback for $Q = 100$ and $F < 0$ (upper panel) or $F > 0$ (lower panel). Conventions are the same as in Fig. 12.

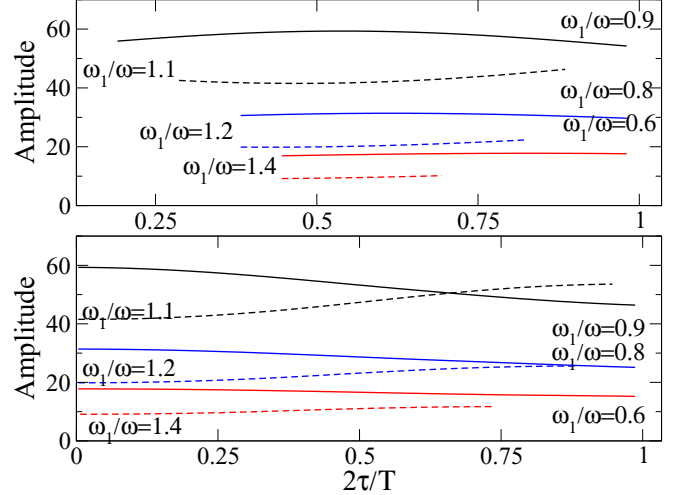


FIG. 14. Comparison of the amplitude of oscillation of oscillators with velocity feedback (upper panel) and position feedback with $F > 0$ (lower panel) for fixed values of the angular frequency of the external force. Both oscillators have $Q = 100$.

here $\tau < T/2$). For these values, every solution of Eq. (2) is asymptotically stable (at least for large Q).

D. External harmonic force and position feedback

In the case of oscillators with a negative feedback based on position, the results we obtain are very similar to the ones presented above for oscillators with velocity feedback but “shifting” the delay by a quarter of a period. The upper panel of Fig. 13 shows the entrainment range in terms of τ (compare with Fig. 12, the equivalent for the velocity feedback oscillator).

More surprisingly, when positive feedback based on position is allowed, the system can be entrained by an external force, even though it cannot oscillate autonomously, as shown in Sec. III. As a function of the delay, the entrainment range is even larger than the entrainment range for oscillators with velocity feedback (see the lower panel of Fig. 12). We also find that the amplitude of the resulting oscillations is similar to the amplitudes obtained with velocity feedback oscillators, and that also in this case the dependence on τ is rather weak (see Fig. 14).

V. CONCLUSIONS

In this article, we have analyzed a simple model of a feedback oscillator driven by an external oscillatory force, focusing on the effects of introducing a delay in the feedback function. To do this, we have obtained an expression for the periodic trajectories of the system, and we have performed an analysis of the asymptotic stability of such solutions. We were interested in particular in characterizing the entrainment region of the oscillator, i.e., the region of parameter space where it can have stable periodic trajectories with the same frequency as the driving force. The criteria obtained can be applied to many oscillatory driving functions, but we have provided here

an example of its usefulness by applying them to the analysis of a system driven by a harmonic external force.

Even though it is well known that the maximal response of most self-sustained oscillators appears when the delay between the signal and the feedback is a quarter of the period (see, e.g., [12,15,16]), we find that when the oscillator is driven by an external force, things can be rather different. Both for velocity- and position-based feedback, we found that the entrainment range is largest for delay values for which the unforced system does not have the maximal response. It can even be largest when the response is minimal for the unforced case. This agrees with the inverse relationship between the amplitude of the unforced system and its range of entrainment found for simple oscillator models [17], which suggests that this could be a common feature in most oscillator systems, regardless of their complexity.

As was to be expected, some of the features of this kind of oscillator are very similar to what happens in a harmonic oscillator. For example, for the unforced system, the resonance appears when ω_1 , the angular frequency of the external signal, coincides with ω , the damped angular frequency of the oscillator, and the amplitude of the oscillations at resonance is proportional to the quality factor Q (for relatively large values of Q). However, when the feedback signal is delayed, the resonance does not appear when $\omega_1 = \omega_\tau$, the angular

frequency of the delayed, unforced system: it appears again at $\omega_1 = \omega$ for all values of the delay. Interestingly, this feature does not depend on the form of the driving function.

It would be interesting to use this formalism to study the case of oscillating external forces that are not harmonic and to understand how the form of the function influences the entrainment range. This can be relevant for biological systems because there are many examples of oscillators that are driven by external signals that are not perfectly harmonic. One extreme example of this is the driving of the circadian oscillator by light pulses (see, e.g., [18]), which can even be randomly distributed throughout the day [19].

To achieve a more realistic model of a micromechanical oscillator, it would be necessary to include cubic nonlinearities in the equation for the resonator. One important example of this is the Duffing equation. Even though this equation cannot be solved analytically in its general form, for relay feedback one only needs the solution for a finite amount of time, and thus a short-time approximation (as in the method of multiple time scales [20]) could be a promising approach.

ACKNOWLEDGMENT

I acknowledge financial support from CONICET through project PIP 11220120100495.

-
- [1] O. Brand, I. Dufour, S. M. Heinrich, and F. Josse, *Resonant MEMS. Fundamentals, Implementation and Application* (Wiley-VCH, Weinheim, Germany, 2015).
- [2] X. L. Feng, C. J. White, A. Haimiri, and M. L. Roukes, *Nat. Nanotech.* **3**, 342 (2008)
- [3] J. M. Nichol, E. R. Hemesath, and L. J. Lauhon, *Appl. Phys. Lett.* **95**, 123116 (2009).
- [4] R. van Leeuwen, D. M. Karabacak, H. S. J. van der Zant, and W. J. Venstra, *Phys. Rev. B* **88**, 214301 (2013).
- [5] F. M. Atay, *Lect. Notes Contr. Inf. Sci.* **273**, 103 (2002).
- [6] J. C. Dunlap, *Cell* **96**, 271 (1999).
- [7] C. H. Johnson, J. A. Elliott, and R. Foster, *Chronobiol. Int.* **20**, 741 (2003).
- [8] A. H. Nayfeh and D. T. Mook, *Nonlinear Oscillations* (Wiley-VCH Verlag GmbH, Weinheim, Germany, 2004).
- [9] G. Wang, T. H. Lee, and C. Lin, *Relay Feedback: Analysis, Identification and Control* (Springer-Verlag, London, 2004).
- [10] K. J. Åström, Oscillations in systems with relay feedback, in *Adaptive Control, Filtering, and Signal Processing*, IMA Vol. Math. Appl. No. 74, edited by K. J. Åström, G. C. Goodwin, and P. R. Kumar (Springer Verlag, Berlin, 1995), pp. 1–25.
- [11] J. N. Blakely, R. M. Cooper, and N. J. Corron, *Phys. Rev. E* **92**, 052904 (2015).
- [12] S. I. Arroyo and D. H. Zanette, *Phys. Rev. E* **87**, 052910 (2013).
- [13] S. H. Strogatz, *Nonlinear Dynamics and Chaos*, Studies in Nonlinearity (Perseus, Reading, MA, 1994).
- [14] A. Pikovsky, M. Rosenblum, and J. Kurths, *Synchronization: A Universal Concept in Nonlinear Science* (Cambridge University Press, Cambridge, 2001).
- [15] L. G. Villanueva, E. Kenig, R. B. Karabalin, M. H. Matheny, R. Lifshitz, M. C. Cross, and M. L. Roukes, *Phys. Rev. Lett.* **110**, 177208 (2013)
- [16] B. Yürke, D. S. Greywall, A. N. Pargellis, and P. A. Busch, *Phys. Rev. A* **51**, 4211 (1995).
- [17] U. Abraham, A. E. Granada, P. O. Westermark, M. Heine, A. Kramer, and H. Herzel, *Mol. Syst. Biol.* **6**, 438 (2010)
- [18] H. Pohl, *Compar. Biochem. Physiol. B* **76**, 723 (1983).
- [19] D. E. F. L. Flôres, B. M. Tomotani, P. Tachinardi, G. A. Oda, and V. S. Valentinuzzi, *PLoS One* **8**, e68243 (2013)
- [20] C. M. Bender and S. A. Orszag, *Advanced Mathematical Methods for Scientists and Engineers* (Springer-Verlag, New York, 1999).